Proceedings of the ASME 2008 International Design Engineering Technical Conferences & Computers and Information in Engineering Conference
IDETC/CIE 2008
August 3-6, 2008, Brooklyn, New York, USA

DETC2008-50033

AN ITERATIVE APPROACH FOR STEADY STATE HANDLING ANALYSIS OF VEHICLES

Indrasen Karogal
Department of Mechanical Engineering
Clemson University
326 Fluor Daniel EIB
Clemson, SC 29634

Beshah Ayalew
Clemson University - International Center for Automotive Research (CU-ICAR)
4 Research Dr. Room 342 CGEC
Greenville, SC 29607

E. Harry Law
Department of Mechanical Engineering
Clemson University
203 Fluor Daniel EIB
Clemson, SC 29634

ABSTRACT

In this paper, we present an iterative approach for analyzing the steady state handling behavior of a two-axled vehicle. This approach computes lateral forces iteratively from two separate submodels. The first submodel is an appropriate tire model that computes per wheel lateral forces as functions of slip angles, from formulations preferably expressed in a non-dimensional format. The second is a lateral weight transfer submodel that computes per-axle lateral force contributions for a given lateral acceleration. The combination then allows for the estimation of the required steer angles for the prevailing lateral acceleration. Subsequent corrections are then applied to take into account steer effects such as roll steer, lateral force compliance steer and aligning moment compliance steer. The usefulness of the approach is demonstrated by comparing simulation results with test data for a small passenger car.

NOMENCLATURE

a_{yg}	lateral acceleration in g's
K_{US}	understeer gradient
δ_f	front steering angle
Δw_{fi}, i=1, 2, 3	weight shifts
w	weight
T	track width
L	wheel base of vehicle
R	radius of curvature during cornering
K_{ϕ}	roll rate (in deg/g)
F_Z	vertical loads on tires
F_y	lateral force
h_{rcf}, h_{rcr}	roll center height front and rear
h_{scg}	height of CG of sprung mass above ground
α_{avg}	average wheel slip angle
C_{α}	cornering Stiffness
C_{γ}	camber Stiffness
l_{1s}, l_{2s}	distance of front and rear sprung mass CG's from CG of vehicle
K_{γ}	roll camber
M_Z	aligning moment
β	sideslip angle
α	slip angle
γ	camber angle
μ	coefficient of friction
$\bar{F}$	non-dimensional lateral Force
$\bar{\alpha}$	non-dimensional Slip angle
w_{ax}	axle weight
lat	lateral force developed by wheel
toe	static toe setting value of vehicle
l_{pt}	pneumatic trail
l_{ut}	mechanical trail
errf, errr	error functions for front and rear axles resp.
ξ	roll steer coefficient
φ	roll angle
A	lateral force compliance steer coefficient
K_{sc}	aligning moment compliance steer coefficient
K_{ack}	Ackermann steering coefficient

The following subscripts will also be used frequently.

SUBSCRIPTS

s	sprung mass
f	front tires
r	rear tires
of	outer front tires
if	inner front tires
uf	unsprung front
ur	unsprung rear
deg	degrees

(i, j) refers to the i^{th} value of slip angle and j^{th} value of lateral acceleration

1. INTRODUCTION

The assessment of vehicle handling often starts with the evaluation of the steady state handling behavior using objective and subjective means [1]. For objective evaluations of steady state handling, the understeer gradient is often used as a quantitative measure of the steady state handling performance of the vehicle. The understeer gradient, denoted by K_{us}, usually computed from constant radius or/and constant speed test methods [2]. Often quasi-steady state approaches of stepping through a range of near-steady cornering maneuvers are also adopted. The validation tests for this work used one of the latter approaches as it allowed faster acquisition of the necessary data for further processing and extraction of steady state regimes.

The understeer gradient K_{US} (in deg/g) determines the steady state handling of a front steered two-axled vehicle according to:

$$\delta_f = 57.3\ \frac{L}{R} + K_{US}.a_{yg} \qquad (1)$$

where a_{yg} is the lateral acceleration in g's, L & R are the track width and radius of turn of the vehicle, respectively, and δ_f is the front road wheel steer angle.

The customary model-based approach for the computation of the understeer gradient involves compiling the contributions of the effects of tire cornering stiffness, tire camber stiffness and roll camber, roll steer, suspension compliance to lateral force and aligning moment, tractive force and caster offset effects. The required data for these approaches are extracted out of kinematics and compliance (K&C) tests conducted on the vehicle. This model-based approach is described in great detail in [2, 6]. The approach gives quick results and is normally good within the linear range of tire behavior. Lateral load transfer effects are considered by linearizing the nonlinear variations of tire cornering stiffness with normal load.

In this paper, we present an iterative approach, developed by E.Harry Law in [6], that exploits the fact that, for a given lateral acceleration, the lateral load transfer can be explicitly computed, and that the nonlinear relationships between tire lateral force, slip angle, and normal load can be readily implemented. The latter aspect is further facilitated by the ready non-dimensionalization of tire data, as described in [3]. Non-dimensionalization of tire data provides accurate and straightforward extrapolation of data to higher or lower loads than those used during the tests [3]. The iterative approach is also briefly mentioned by Genta [7, pages 311-312]. Here, we give a detailed discussion of the iterative approach including a computational flow diagram for a typical implementation.

The rest of the paper is organized as follows. In Section 2, we describe the iterative approach proposed in this paper. In Section 3, we present some comparisons of the approach discussed in the paper with test data and the results of the customary approach. We present the conclusions of the work in Section 4.

2. STEADY STATE HANDLING ANALYSIS: ITERATIVE MODEL

As already pointed out, the customary model for computation of understeer gradient (simply adding the contributions from various steer effects) simplifies effects from lateral weight shift and consequently ignores possible contributions from differences between the inside and outside tire properties. The customary model does not explicitly compute the slip angles and the lateral forces developed at each of the inner and outer tires. The iterative model we present in this section will explicitly compute the lateral forces and slip angles at each tire.

The proposed model uses non-dimensionalized lateral force tire data and calculates per wheel slip angles and lateral forces and compares the per-axle lateral force thus obtained with the per-axle lateral force obtained from a weight shift model. To start off, guess values of slip angles are provided as input, and the slip angles are subsequently corrected iteratively to minimize the difference between the per-axle lateral force given by the nondimensional data and the weight shift model. The method is best described by detailing the necessary steps, as we do below.

1) Start with preparing an input list of vehicle parameters. This includes geometrical parameters such as track width and wheel base, suspension roll stiffnesses, roll centers, CG locations, and the sprung and unsprung masses of the vehicle. These data are essentially the same as the data required for the customary method of steady state handling analysis outlined in [2].

2) Weight shift submodel. This submodel computes the lateral weight shift using vehicle parameters listed above for a given

value of lateral acceleration. This submodel, also discussed in [2] allows for the calculation of the roll angle, roll rate, wheel normal forces and per axle lateral forces corresponding to the given lateral acceleration. The computation is based on the model shown in Fig.1.

The three primary contributions to lateral weight shift [2, 6] are listed here briefly:

2.1. Weight shift proportional to roll center height and track width as given by:

$$\Delta w_{f1} = \left(\frac{w_s * l_{2s}}{T_f}\right) * \left(\frac{h_{rcf}}{T_f}\right) * a_{yg} \quad (2)$$

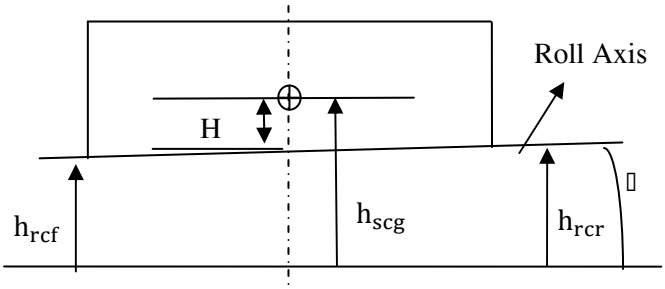

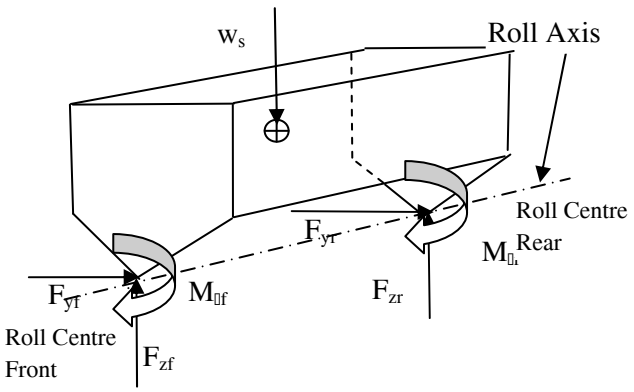

Figure 1 A Free Body Diagram Of The Sprung Mass Of A Two-Axled Vehicle In Steady State Cornering [6]

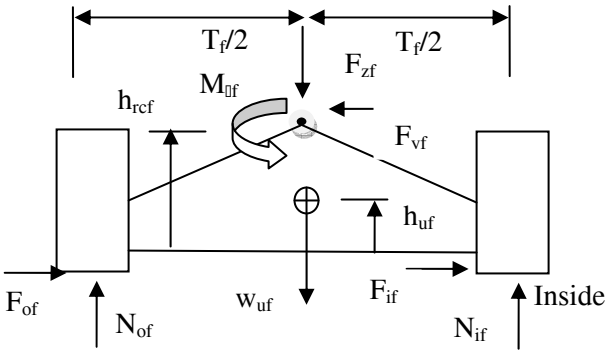

Figure 2 Free body diagram of unsprung mass of two-axled vehicle in steady state cornering (Front View) [6]

2.2 Weight shift proportional to product of roll rate and roll stiffness as given by:

$$\Delta w_{f2} = \left(\frac{K_{\phi f}}{(K_{\phi f} + K_{\phi r} - w_s * H)}\right) * \left(\frac{w_s * H}{T_f}\right) * a_{yg} \quad (3)$$

where H is the height of the CG of sprung mass above the roll axis, as shown in Fig.1, is computed from:

$$H = h_{scg} - h_{rcf} - l_{1s} * \left(\frac{(h_{rcr} - h_{rcf})}{L}\right) \quad (4)$$

2.3. Weight shift proportional to CG height of unsprung mass as given by:

$$\Delta w_{f3} = \left(\frac{w_{uf} * h_{uf}}{T_f}\right) * a_{yg} \quad (5)$$

The total lateral weight shift for the front tires is given by:

$$\Delta w_f = \Delta w_{f1} + \Delta w_{f2} + \Delta w_{f3} \quad (6)$$

Proceeding similarly, the total lateral weight shift for the rear tires is given by:

$$\Delta w_r = \left(\frac{w_s * l_{1s}}{T_r}\right) * \left(\frac{hrc_r}{T_r}\right) * a_{yg} + \left(\frac{K_{\phi r}}{(K_{\phi r} + K_{\phi r} - w_s * H)}\right) * \left(\frac{w_s * H}{T_r}\right) * a_{yg} + \left(\frac{w_{ur} * h_{ur}}{T_r}\right) * a_{yg} \quad (7)$$

Equations (2-7) are obtained from the equations of motion for the sprung mass and the unsprung masses, as shown in Figs 1 and 2, respectively.

The inside and outside normal loads are computed from:

$$F_{zif} = 0.5 * \left(w_{uf} + \frac{w_s * l_{2s}}{L}\right) - \Delta w_f \quad (8)$$

$$F_{zof} = 0.5 * \left(w_{uf} + \frac{w_s * l_{2s}}{L}\right) + \Delta w_f \quad (9)$$

$$F_{zir} = 0.5 * \left(w_{ur} + \frac{w_s * l_{1s}}{L}\right) - \Delta w_r \quad (10)$$

$$F_{zor} = 0.5 * \left(w_{ur} + \frac{w_s * l_{1s}}{L}\right) + \Delta w_r \quad (11)$$

The roll gain or roll rate (in deg/g) of the sprung mass is [2]:

$$K_\phi = \left(\frac{w_s * H}{(K_{\phi f} + K_{\phi r} - w_s * H)}\right) * \left(\frac{180}{\pi}\right) \quad (12)$$

The roll angle (in deg) for a given lateral acceleration is then, given by

$$\phi_{deg} = K_\phi * a_{yg} \quad (13)$$

The front and rear axle lateral forces are given by

$$lat_f = w_{axf} * a_{yg} \quad (14)$$

$$lat_r = w_{axr} * a_{yg} \quad (15)$$

3) Tire submodel.

3.1. A suitable tire submodel relating lateral force to the side slip angle, camber angle and normal load is implemented. In this work, we used a Pacejka (Magic Formula) formulation detailed in Appendix A. The inputs to this model are wheel normal loads obtained from the weight shift submodel discussed above and camber angles. For a given slip angle, camber angle, and normal load, the model computes the lateral force and in turn the cornering stiffness C_α and camber stiffness C_γ, each as functions of F_Z and a_{yg}.

3.2. We then fit polynomials relating C_α to F_Z and C_γ to F_Z. This allows us to calculate the prevailing stiffnesses C_α, C_γ for each tire of the vehicle for the above determined normal loads corresponding to the lateral acceleration a_{yg}.

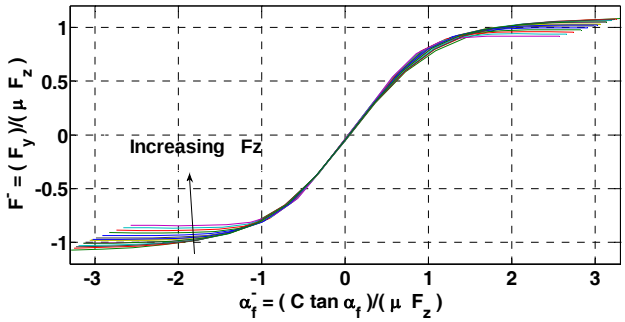

Figure 3 Non-dimensional parameters $\bar{F}$ vs $\bar{\alpha}$ for different vertical wheel loads

3.3. Then a non-dimensional tire submodel is set up. Inputs to this submodel are the C_α for the given lateral acceleration, and the polynomial fits of C_α to F_Z determined in step 3.2. The outputs are Radt non-dimensional parameters $\bar{F}$ and $\bar{\alpha}$ given by:

$$\bar{F} = \frac{F_y}{\mu F_z} \tag{16}$$

$$\bar{\alpha} = \frac{C_\alpha \tan\alpha}{\mu F_z} \tag{17}$$

where μ is the adhesion coefficient of the road surface, F_z is normal wheel load and C_α is the cornering stiffness. Figure 3 shows the plots of $\bar{F}$ Vs $\bar{\alpha}$ for 15 different values of normal load (F_z). A polynomial function can be fitted to this curve. In the present case, a 3rd order (cubic) polynomial fit was used. This fitted curve will be used to compute the lateral forces in the iterative submodel described below. Curve fitting can also be achieved using the Magic Formula formulation as described in references [3, 4] or by using different order polynomials.

4) Iterative submodel.

The inputs to this submodel are lateral acceleration and slip angles. The outputs are the average slip angle for each of front and rear tires and the per wheel lateral forces developed. This iterative process, whose flow diagram is depicted in Fig B1 of Appendix B, can be described in the following sequence:

4.1. Define the range of operation of the vehicle and initialize the iterative process. This includes setting minimum and maximum values of slip angles and lateral acceleration. Suppose the number of data points of lateral acceleration (a_{yg}) and slip angles for outside tires (α_0) be N (i=1, 2… N) and S (j=1, 2… S), respectively. That is:

$$a_{ygmin} \le a_{yg} \le a_{ygmax} \tag{18}$$

$$\alpha_{ofmin} \le \alpha_{of} \le \alpha_{ofmax} \tag{19}$$

The two variables can be initialized as follows:

$$a_{yg}(i) = a_{ygmin} \tag{20}$$

$$\alpha_{of}(j) = \alpha_{ofmin} \tag{21}$$

4.2. Calculate the slip angle, $\alpha_{if}(j)$, for the inside wheel based on $\alpha_{of}(j)$, the Ackermann angle and static toe. Ackerman steering geometry defines the following relationship:

$$\cot(\delta_{of}) - \cot(\delta_{if}) = K_{ack} * \frac{T_f}{L} \tag{22}$$

We are interested in the differences between the inner and outer steering angles as well as between the wheel slip angles. Also often, the range of these angles in radians is very small. Thus, $\delta_{of} \approx \delta_{if}$. As we are starting with assumed values of small angles in the iterative loop, we can safely assume that the relationship defined by equation (22) holds for wheel slip angles as well.

Hence, the slip angle of inside wheel can be given by:

$$\alpha_{if}(j) = \tan^{-1}\left\{\frac{\tan(\alpha_{of}(j))}{\left(1 - K_{ack} * \frac{T_f}{L}\right) * \tan(\alpha_{of}(j))}\right\} \tag{23}$$

Applying static toe settings, the slip angles of inside and outside front wheels can be calculated , respectively, as:

$$\alpha_{inf}(j) = -toe_f * \left(\frac{\pi}{180}\right) + \alpha_{if}(j) \tag{24}$$

$$\alpha_{outf}(j) = +toe_f * \left(\frac{\pi}{180}\right) + \alpha_{of}(j) \tag{25}$$

4.3. Calculate non-dimensional slip angles $\bar{\alpha}_{of}(i,j)$ and $\bar{\alpha}_{if}(i,j)$ and the corresponding non-dimensional lateral force $\bar{F}_{of}(i,j)$ and $\bar{F}_{if}(i,j)$ for each wheel from the polynomial fits of Radt non-dimensionalization submodel using Eq (16) & (17), as explained in step 3.3.

4.4. Calculate the dimensional lateral force F_{yof} and F_{yif} for each wheel using the relationship:

$$F_{yif}(i,j) = \bar{F}_{if}(i,j) * \mu * F_{zif}(i) + C_{\gamma if}(i) * K_{\gamma if} * \Phi(i) \tag{26}$$

$$F_{yof}(i,j) = \bar{F}_{of}(i,j) * \mu * F_{zof}(i) + C_{\gamma of}(i) * K_{\gamma of} * \Phi(i) \tag{27}$$

The resulting per-axle lateral force is given by:

$$F_{yf}(i,j) = F_{yof}(i,j) + F_{yif}(i,j). \tag{28}$$

Also, we calculate the force error function:

$$errf(i,j) = \left|\frac{[F_{yf}(i,j) - latf(i)]}{latf(i)}\right| \tag{29}$$

This error determines the deviation of the front-axle lateral force F_y determined by Eq (28) from the one calculated from Eq (14) of the weight shift submodel.

4.5 Calculate the average front wheel slip angle by:

$$\alpha_{favg}(j) = 0.5 * [\alpha_{of}(j) + \alpha_{if}(j)] \tag{30}$$

At this point, we update the computed per-axle slip angle and the error function.

$$\alpha_{favg}(i) = \alpha_{favg}(j) \quad (31)$$

$$errf(i) = errf(i, j) \quad (32)$$

4.6 For a pre-defined acceptance limit (say 1%), we check whether the error function errf(i) is less than or equal to this value. If this is met, we increment the lateral acceleration (and the index i). That is, $a_{yg}(i) = a_{yg}(i + 1)$. Then we go back to step 4.3 and repeat all the steps from step 4.3 through step 4.6 for this data point of a_{yg}.

Wherever errf(i) is greater than the limit, increment the slip angle, that is, $\alpha_0(j) = \alpha_0(j + 1)$ and go back to step 4.4 and repeat through 4.6 for this data point of wheel slip angle.

Iterating in this way, for each data point $a_{yg}(i)$, a value of $j = j^*$ and hence a corresponding $\alpha_0{}^*(j)$ is determined that gives errf(i) within the acceptance limit. In the case of multiple occurrences of j^* values, the lower value of j^* is considered. Also, the corresponding average front wheel slip angles $\alpha_{favg}(i) = \alpha_{favg}(j^*)$ are stored as a function of a_{yg}.

5) The iterative process is carried out for the rear tires in a similar manner with the corresponding parameters for rear tires. The major change is in the calculation of the slip angle of the inside wheel from that of the outside wheel (as Ackermann steering geometry relationship is not applicable for the rear tires in a front steered vehicle). Instead we proceed with the estimates:

$$\alpha_{inr}(j) = -toe_r * \left(\frac{\pi}{180}\right) + \alpha_{or}(j) \quad (33)$$

$$\alpha_{outr}(j) = +toe_r * \left(\frac{\pi}{180}\right) + \alpha_{or}(j) \quad (34)$$

6) Apply corrections due to steer effects.

The steer angle, front and rear axle slip angles and the car body sideslip angle, β, are related by [2,6]:

$$\alpha_{favg} + \frac{a}{R} = \delta + \beta \quad (35)$$

$$\alpha_{ravg} = \frac{b}{R} + \beta \quad (36)$$

where R is the radius of curvature of the vehicle during cornering.

From Eq (35) and (36) the nominal steer angle is given by:

$$\delta_{fuc} = \left(\frac{L}{R}\right) + (\alpha_{favg} - \alpha_{ravg}) \quad (37)$$

At this point, we incorporate the effects of roll steer, lateral force compliance steer and the offset of lateral forces due to pneumatic and mechanical trails by adding correction terms in the expression of the front wheel steer angle. In addition, compliance in the steering system adds caster angle and aligning torque effects to the overall steer effects, as explained in [2, pages 294-295]. These effects would be considered during the computation of understeer gradient w.r.t steering wheel angle. The expressions and corresponding sign conventions adopted for introducing the other steer effects are listed in Table 1. The resulting front wheel steer angle required is:

$$\delta_f = \delta_{fuc} + +\delta_r + \Delta\alpha_f = \left(\frac{L}{R}\right) + (\alpha_{favg} - \alpha_{ravg}) + \delta_r + \Delta\alpha_f \quad (38)$$

Where δ_r is the rear axle steer correction computed by:

$$\delta_r = -(\xi_r \varphi - A_r F_{yr} + K_{scr} l_{ptr} F_{yr}) \quad (39)$$

And $\Delta\alpha_f$ is the correction to δ_f given by:

$$\Delta\alpha_f = \xi_f \varphi - A_f F_{yf} + K_{scf}(l_{ptf} + l_{mt}) F_{yf} \quad (40)$$

Using (39) and (40) in (38), we get:

$$\delta_f = \left(\frac{L}{R}\right) + (\alpha_{of} - \alpha_{or}) + (\xi_f - \xi_r)\Phi - (A_f F_{yf} - A_r F_{yr}) + K_{scf}(l_{ptf} + l_{mt}) F_{yf} - K_{scr} l_{ptr} F_{yr} \quad (41)$$

One of the terms appearing in the above correction is the pneumatic trail, l_{pt}. The pneumatic trail is computed from:

$$M_z = -l_{pt} * F_y \quad (42)$$

where M_z the aligning moment, l_{pt} is the pneumatic trail for the respective tires, and F_y is the lateral force.

7. Computing the Understeer Gradient (K_{US})

After repeating the above procedure (steps 1-6) for each data point of lateral acceleration (a_{yg}), from Eq. 1, the understeer gradient, K_{US}, in deg/G at a given lateral acceleration, say $a_{yg} = a$, is computed as the slope of road wheel understeer Vs a_{yg} curve at $a_{yg} = a$:

$$K_{us} = \left[\frac{d}{d\, a_{yg}} (RWUS)\right]_{a_{yg}=a} \quad (43)$$

where road wheel understeer (RWUS) is defined as:

$$RWUS = \left(\delta_f - 57.3 \frac{L}{R}\right) \quad (44)$$

Table 1 Expressions and Adopted Sign Conventions of Various Steer Effects on Vehicle		
Expression	**Description and Effect on Vehicle**	**Sign Convention**
$\xi_f \varphi$	Roll steer; steer of front axle is out of right hand turn - an understeer effect	> 0
$A_f F_{yf}$	Lateral force compliance steer; steer of front axle is into right hand turn - an oversteer effect	> 0
$K_{scf}(l_{ptf} + l_{ut})F_{yf}$	Aligning moment compliance steer; steer of front axle is out of right hand turn - an understeer effect	> 0
$\frac{a_y (Wl_{ptf})}{C_{\alpha f}}$	Aligning torque due to offset of lateral forces; steer of front axle is out of right hand turn - an understeer effect	> 0
$\xi_r \varphi$	Roll steer; steer of rear axle is out of right hand turn - an oversteer effect	> 0
$A_r F_{yr}$	Lateral force compliance steer; steer of rear axle is out of right hand turn - an understeer effect	> 0
$K_{scr}(l_{ptr})F_{yr}$	Aligning moment compliance steer; steer of rear axle is into right hand turn-an oversteer effect	> 0
$\frac{a_y (Wl_{ptr})}{C_{\alpha r}}$	Aligning torque due to offset of lateral forces; steer of front axle is out of right hand turn-an understeer effect	> 0

3. COMPARISON WITH TEST DATA

To validate the approach, tests were conducted on a small passenger car and the iterative approach discussed in this paper was used to carry out a steady-state handling analysis on the vehicle. Two steady state performance metrics were used for this comparison: the understeer gradient and the body slip angle response for a given lateral acceleration.

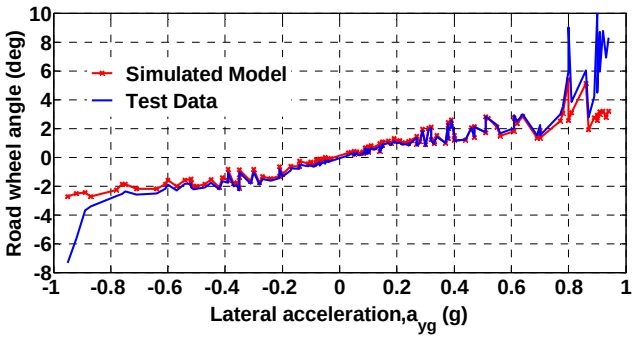

Figure 4 Road wheel steer angle vs. lateral acceleration.

Figure 4 shows a plot of road wheel angle vs a_{yg} for a curb + driver load case as obtained from iterative simulation model and test data. It can be seen that there is a very close match between the test and simulation results, particularly with in region of a_{yg} = - 0.4 g's to 0.4 g's.

Figure 5 shows a comparison of the road wheel understeer (RWUS) computed from test data against the one computed by using the iterative model over the full range of the lateral acceleration a_{yg}. The understeer gradient, as defined by equation (43) is calculated as the slope of the simulated model results over the region of a_{yg} = - 0.4 to 0.4 g's. Over this range the slip angle varies linearly with lateral acceleration. Again, it can be seen that there is a very good match between the test and model results, especially in the linear region of a_{yg} = - 0.4 to 0.4 g's.

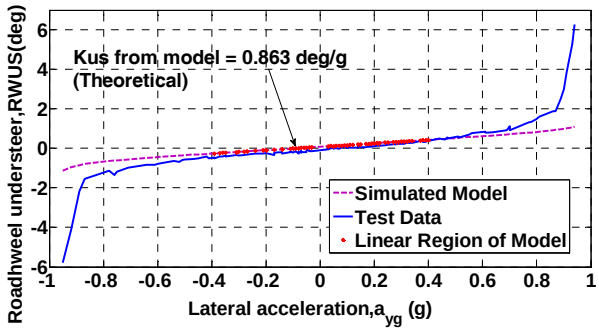

Figure 5 Comparison of road wheel understeer (RWUS) from model and test data

Table 2 shows the comparison of results for the understeer gradient computed using the customary and the iterative modeling approaches and that computed from measured vehicle test data. As mentioned in Section 2, step 6, the compliance in the steering system, if taken into account, will further increase the understeer gradient of the system obtained by either of the two models (iterative and customary). We believe that the compliance steer contribution of the bushings and the portion of the rack between the road wheels and actual rack-displacement sensor (used for measuring road wheel steer angle during testing) location, as well as the small angle approximations in interpreting sensor outputs into angles, account for some of the difference between the test results and the model results. However, we can clearly see the significant

improvement obtained by using the iterative method over the customary approach.

Table 2. COMPARISON OF UNDERSTEER GRADIENT FROM TEST DATA, CUSTOMARY MODEL AND ITERATIVE MODEL

Load cases	K_{us} from Test Data (deg/g)	K_{us} from Customary Model (deg/g)	K_{us} from Iterative Model (deg/g)
Curb+Driver clockwise test runs	1.039	0.600	0.863
Curb+Driver counterclockwise test runs	1.120	0.600	0.860

Figure 6 shows a comparison of variations of the body side slip angle (β) with lateral acceleration (a_{yg}) for the simulated model and processed test track data. For the test data, the body side slip angle β (at vehicle C.G.) was obtained by transforming rear bumper located slip angle sensors. Within the region of a_{yg} = - 0.4 g's to 0.4 g's, a close match was observed between the test and simulation results. This is the expected region of linearity for the method (its use of concepts of cornering and camber stiffnesses) adopted and as such the match is considered satisfactory for this region.

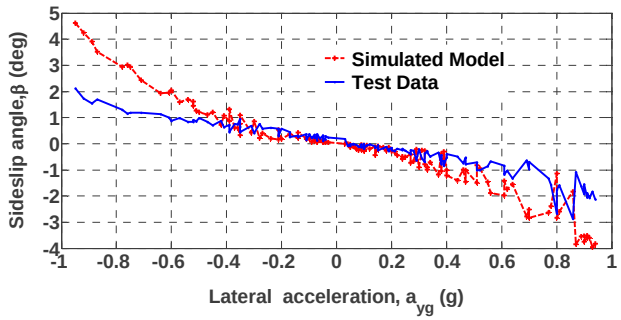

Figure 6 Body sideslip angle vs. lateral acceleration from model & test data

We note that, in order to compute the body slip angle response using the customary approach, one has to first compute the understeer gradient. The iterative approach computes the slip angle response more directly.

4. CONCLUSIONS

In this paper, we outlined an iterative procedure for characterizing the steady state handling performance for a two-axled vehicle. The approach computes the prevailing lateral forces corresponding to a given lateral acceleration by using two submodels. The first submodel is a lateral force tire submodel that gives the lateral force as a function of slip angle expressed in a non-dimensional format. The second is a lateral weight transfer submodel that computes per-axle lateral force contributions for a given lateral acceleration. The method then iterates between the two submodels to determine the required steer angle for a given lateral acceleration. Subsequent corrections are then applied to take into account other elasto-kinematic steer effects such as roll steer, lateral force compliance steer and aligning moment compliance steer, as well caster and pneumatic trail offset effects.

We applied the iterative method for the steady state handling analysis of a small passenger car. Comparisons with the customary approach showed that the iterative method gives understeer gradient results closer to those computed from test data. We also observed that, for a sizeable range of lateral accelerations, the iterative method gives a direct prediction of the body side slip angle as well.

In conclusion, the iterative method has a very good potential for improving steady state analysis efforts. One such effort may be analyzing the sensitivity of the understeer gradient to tire properties. We are currently pursuing such an application of the iterative method.

Acknowledgements:

The authors would like to acknowledge the team at Michelin including Tim Rhyne, Jon Henderson and Norm Frey for providing test track and the K & C test data for the comparisons presented here.

APPENDIX A: PACEJKA TIRE MODEL: LATERAL FORCE AND ALIGNING TORQUE

Name	Symbol	Units
Lateral force	F_y	N
Self aligning torque	M_Z	N.m
Slip angle	α	deg
Vertical load	F_Z	kN
Camber angle	γ	deg

1) Lateral Force Equations

$$F_y = D * \sin(C * \tan^{-1}(B * \varphi)) + S_V \quad (45)$$

$$\varphi = (1 - E) * (\alpha + S_H) + \left(\frac{E}{B}\right) * \tan^{-1}(B * (\alpha + S_H)) \quad (46)$$

$$D = (a_1 * F_Z + a_2) * F_Z \quad (47)$$

$$BCD = \left(a_3 \sin\left(2 * \tan^{-1}\left(\frac{Z}{a_4}\right)\right) * (1 - a_5 * |\gamma|)\right) \quad (48)$$

$$B = \left(\frac{BCD}{C*D}\right) \quad (49)$$

$$C = a_0 \quad (50)$$

$$E = (a_6 * F_Z + a_7) * F_Z \quad (51)$$

$$S_H = a_8 * \gamma + a_9 * F_Z + a_{10} \quad (52)$$

$$S_V = (a_{112} * F_Z + a_{111}) * F_Z * \gamma + a_{12} * F_Z + a_{13} \quad (53)$$

2) Aligning Moment Equations:

$$M_Z = D * \sin(C * \tan^{-1}(B * \varphi)) + S_V \quad (54)$$

$$D = (c_1 * F_Z + c_2) * F_Z \quad (55)$$

$$BCD = (c_3 * F_Z + c_4) * F_Z * e^{-(c_5 * F_Z)} * (1 - c_6 * |\gamma|) \quad (56)$$

$$B = \left(\frac{BCD}{C*D}\right) \quad (57)$$

$$E = (c_7 * {F_Z}^2 + c_8 * F_Z + c_9) * (1 - c_{10} * |\gamma|) \quad (58)$$

$$S_H = c_{11} * \gamma + c_{12} * F_Z + c_{13} \quad (59)$$

$$S_V = (c_{14} * F_Z + c_{15}) * F_Z * \gamma + c_{16} * F_Z + c_{17} \quad (60)$$

The parameters a_1 through c_{17} are numerical constants determined by flat track tire tests.

APPENDIX B: FLOW DIAGRAM FOR ITERATIVE METHOD

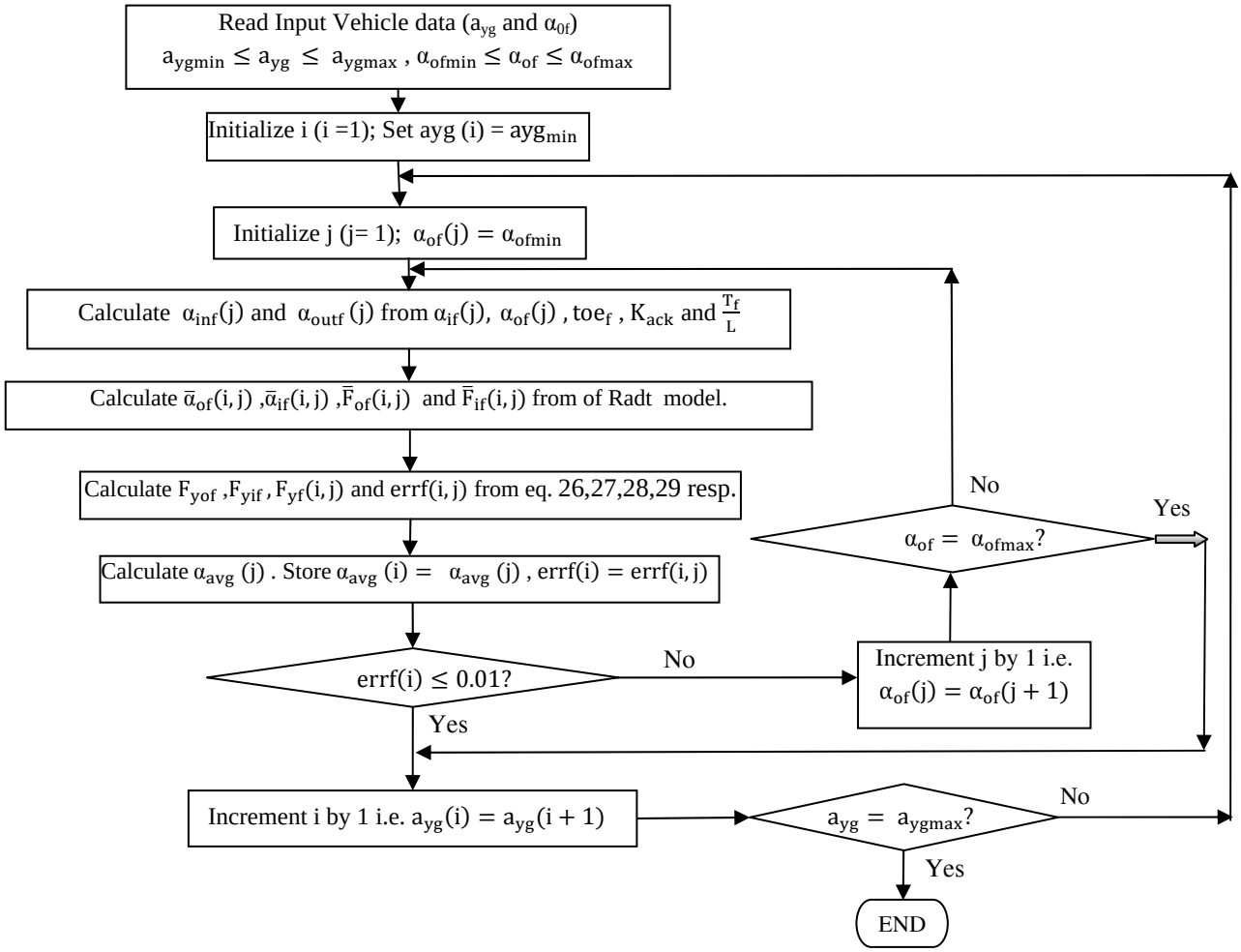

Figure B1 Flow Diagram for the Iterative Method

5 REFERENCES

1. Metz L.D., "What Constitutes Good Handling?", SAE Technical Paper no. 2004-01-3532

2. Gillespie, T. D., Fundamentals of Vehicle Dynamics, SAE, 1992.

3. Radt, Hugo S., Jr., "An Efficient Method for Treating Race Tire Force-Moment Data", SAE Technical Paper no. 942536, 1994.

4. Bakker, E., Pacejka H.B. and Lidner L, "A New Tire model with an Application in vehicle dynamic studies," SAE Technical paper number 890087.

5. Pacejka H.B., Tire and Vehicle Dynamics, 2nd ed., SAE, 2002.

6. Course Notes for ME653- Dynamic Performance of Vehicles, Chapters 10-11, by Prof. E.H. Law, Clemson University, Department of Mechanical Engineering.

7. Genta G., Motor Vehicle Dynamics, Modeling and Simulation, Series on Advances in Mathematics for Applied Sciences-Vol.43